

Negative Magnetoresistance in Andreev Interferometers

W. Belzig

Department of Physics and Astronomy, University of Basel, Klingelbergstr. 82, 4056 Basel, Switzerland

R. Shaikhaidarov and V. V. Petrashov

Department of Physics, Royal Holloway, University of London, Egham, Surrey TW20 OEX, United Kingdom

Yu. V. Nazarov

Department of Applied Physics, Delft University of Technology, Lorentzweg 1, 2628CJ Delft, Netherlands

We consider transport in a diffusive cross-shaped Andreev interferometer geometry, both theoretically and experimentally. A strong and unexpected modulation of the conductance with the superconducting phase is found. In particular, a reversed resistance vs. phase difference is predicted, where the resistance is *decreased* by a phase gradient. A comparison of our quasiclassical calculation with experimental data shows quantitative agreement if we account for diamagnetic screening.

Quantum mechanical interference effects can be ideally studied in heterostructures of normal metals and superconductors. Large conductance oscillations in structures containing loops threaded by a magnetic flux have been predicted and observed [1, 2, 3, 4, 5, 6, 7, 8]. The origin of these oscillation is the phase coherence between Andreev coupled electron-hole pairs, which can be maintained over large distances of the order of μm , making their observation in microstructured devices accessible [9, 10, 11, 12]. Since the origin of these oscillation are superconducting correlations, they are usually suppressed by a magnetic field, i.e. these devices show a positive magnetoresistance. This trend can be reversed by means of tunnel junctions, in which case the conductance is strongly reduced due to a suppression of the low energy density of states leads. Obviously, the suppression of superconducting correlations then leads to a decreased resistance [13]. Thus, one would expect that a magnetic field drives the resistance towards its normal state value, no matter in what direction this actually is.

Here we report on a theoretical calculation and an experimental measurement of the magnetotransport of a purely diffusive heterostructure, which shows a negative magnetoresistance due to an subtle interference effect. This is surprising, since generally one would expect, that both finite energies and a phase gradient would lead to a destructive interference, diminishing the proximity effect. Thus, although the conductance shows the so-called reentrance effect as function of temperature, one would not expect a phase gradient to reverse the temperature effect. In the present Letter we study a geometry, in which a separation of the energy scales responsible for these two effects result in a negative magnetoresistance.

We will first describe the theoretical approach, which predicts a negative magnetoresistance for small magnetic flux. To obtain the experimentally observed fully inverted resistance oscillations, we will have to include diamagnetic screening in the superconducting loop imposing the phase difference. This allows us to obtain excellent

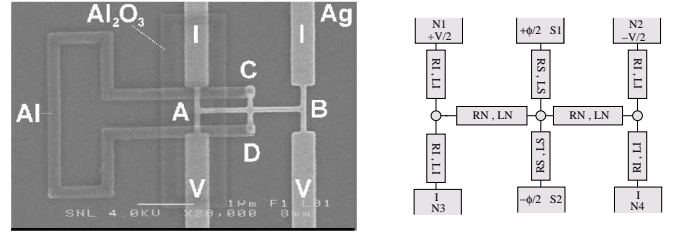


FIG. 1: Geometry of experimental setup and the theoretical model. The left picture shows a micrograph of the experimental layout. The resistance of the horizontal Ag wire is measured in 4-terminal configuration by current(I)- and voltage(V)-probes attached to points A and B. In the middle two superconducting mirrors C and D made from Al are attached by Ag wires. The superconducting mirrors are connected to loop threaded by a magnetic flux, which allows to vary the phase difference between C and D. Theoretically we model the experimental setup by the structure shown in the right panel. The resistors R_S , R_N and R_I model the respective Ag-wires of length L_S , L_N and L_I .

agreement using parameters determined from the experiment independently. We note that this agreement is contrary to the claim in Ref. [14], in which a similar experimental layout was studied. It was however claimed, that the experimental observations can not be explained within the 'standard theory' of the mesoscopic diffusive proximity effect. Here, we show that these observations are in perfect agreement with the 'standard' quasiclassical theory.

The system we study is shown in Fig. 1. The left part shows the experimental setup and the right shows the theoretical model structure. The resistance of the vertical piece of normal metal is to be measured. Each part (left and right) of this vertical wire has a resistance R_N and a length L_N . The reservoirs inducing superconductivity (S1 and S2) are attached to the middle of the wire by normal resistors of length L_S and resistance R_S . The actual measurement of the resistance is performed in a

4-terminal geometry by attaching current and voltage probes (N1-N4) through resistors of length L_I and resistance R_I . Note, that these probes have to be included into the modeling in contrast to normal systems. In a proximity effect structure, the properties of these probes matter, since they modify the equilibrium properties (i.e. the density of states and therefore the energy- and space-dependent conductivity of the system).

The calculation of the resistance of the structure depicted in Fig.1 has been performed numerically, along the lines of Ref. [7, 15] using the quasiclassical formalism[16]. From the spectral Usadel equation the local energy-dependent conductivity is extracted via

$$\sigma(E, x) = \frac{\sigma_N}{4} \text{Tr} [\hat{1} - \hat{\tau}_z \hat{g}_R \hat{\tau}_z \hat{g}_A] . \quad (1)$$

Here σ_N is the normal state conductivity and $\hat{g}_{R,A}$ are retarded and advanced Nambu Green's functions obeying the Usadel equation (see Ref. [15] for a definition). The solution of the kinetic equation yields for the measured 4-terminal resistance

$$R^{-1} = \int \frac{dE}{4T \cosh^2(\frac{E}{2T})} \left(\int_0^{L_N} \frac{dx}{\sigma(E, x)} \right)^{-1} . \quad (2)$$

Similarly we can find the supercurrent in equilibrium as

$$I_S = \frac{\sigma}{8} \int dE \text{ImTr} \left[\hat{\tau}_z \hat{g}_R \frac{\partial}{\partial y} \hat{g}_R \right] \tanh \left(\frac{E}{2T} \right) . \quad (3)$$

These expressions show, that the 4-Terminal configuration indeed measures the resistance of the vertical branch only. However, due to the proximity effect the spectral conductivity $\sigma(E, x)$ depends also on the properties of the current and voltage leads. As a consequence this will also lead to a strongly increased supercurrent for temperatures at which these branches are probed, as we demonstrate below.

We now discuss the concrete theoretical results. The parameters, that we have chosen correspond to the experimental setup shown in the left panel of Fig. 1. The dimensions are $L_N = 1000\text{nm}$, $L_S = 225\text{nm}$ and $L_I = 800\text{nm}$, where L_I is taken a little bit larger than in the experiment to account for the proximity effect into the wider ("lead") regions of the experiment. For the connectors to the superconductor we have taken the distance between the central point and the closest point of the superconductor. Taking the experimental value of the diffusion constant $D \approx 80\text{cm}^2/\text{s}$, we find for the Thouless energy $E_N = \hbar D/L_N^2 = 57\text{mK}k_B$. The branch connecting the two superconductors directly has correspondingly $E_S = \hbar D/4L_S^2 = 280\text{mK}k_B$ (we took the full length, since this is mainly used in literature to characterize SNS junctions). In the calculation we have assumed a temperature independent superconducting gap corresponding to $\Delta/k_B = 2\text{K}$.

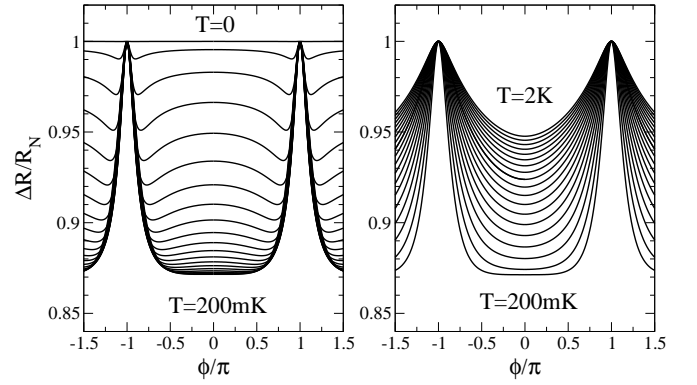


FIG. 2: Resistance versus phase difference. Right plot: resistance oscillations for temperatures between 200mK and 2K in steps of 100mK. Left plot: resistance oscillations for temperatures from 0 to 200mK in steps of 10mK. The form of the oscillations at temperatures above 200mK are as expected, i.e. the resistance monotonously increases between 0 to π . Below 200mK the phase dependence changes qualitatively. In particular for small phase difference the magnetoresistance is negative.

Let us now turn to the phase dependent resistance of the vertical branch, measured in 4-point configuration through the leads N1-N4. The resistance oscillations for a large range of temperatures are shown in Fig. 2. Following the temperature dependence of the resistance for zero phase difference, we observe the usual reentrance behaviour, with a maximal suppression of about 13% at a temperature around 200mK. At a phase difference of π (or any odd multiple), the proximity effect is completely suppressed for all temperatures. At temperatures above 200mK the resistance vs. phase oscillation are similar to that predicted previously [6, 7, 8] and found experimentally[1, 5]. However, below 200mK the oscillations change qualitatively. Whereas the resistance increases monotonically starting from zero phase difference for the larger temperatures, it *decreases* first for the lower temperatures. Only close to half-integer phases the resistance increases again. At half-integer flux the resistance is always equal to the normal state value, as it should be.

Obviously, such a strong change of the phase-dependence should also affect other transport properties, for example the temperature- and the phase-dependence of the supercurrent. The theoretical results are shown in the inset of the left panel of Fig. 3. Note that, for simplicity, we have not included the temperature dependence of the superconducting gap. Therefore, the supercurrent is finite above the experimental critical temperature of $\approx 1.4\text{K}$. The critical current strongly increases below a temperature close to E_S . At higher temperatures the critical current depends only weakly on the temperature (the exponential decrease $\sim \exp(-\sqrt{k_B T/E_S})$ sets in only at much larger temperatures). The strong increase

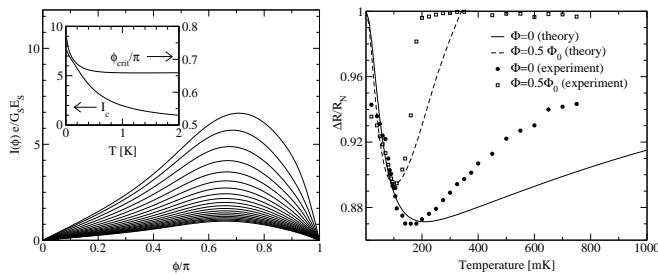


FIG. 3: Left panel: Supercurrent phase relation (main) and critical current/critical phase (inset). The non-sinusoidal current phase relation is plotted for temperatures from 100mK to 1K in steps of 100mK (from bottom to top). For phase differences around $3\pi/4$ the increase is strongest. The inset shows the temperature dependence of the critical current, together with the phase at which it is reached. Both quantities show a strong variation below 1K. Right panel: resistance versus temperature for integer and half-integer external flux. The lines are theoretical results and the symbols correspond to the experimental data. For integer flux both, experiment and theory, show the usual reentrance behaviour. For half-integer flux, the resistance decreases from the normal state resistance below a temperature of about 400mK. At lower temperatures it drops even below the resistance for integer flux. We attribute the saturation of the experimental resistance at very low temperatures to heating effects. The best fit of the resistance for half-integer flux was obtained for a screening parameter $\gamma = 0.005e/G_N E_N$.

is related to the influence of the vertical branch. As superconducting correlation become strong in this branch, the pair breaking influence of normal lead gets effectively suppressed. Accordingly the supercurrent increases drastically. The phase-difference, for which the critical current is reached, shifts from 0.65π up to 0.8π in the same temperature interval. In the left panel of Fig. 3 we show the current-phase relation in a temperature interval between 100mK and 2K. It is clearly non-sinusoidal and also changes qualitatively at low temperatures.

Summarizing these theoretical results, we have observed a rather surprising phase-dependence of transport properties in a multi-terminal diffusive heterostructure. However, the experimental results, shown in the left column of Fig. 4, are quite different. The reason, as we will quantify below, is the diamagnetic screening in the superconducting loop. The applied magnetic flux induces a supercurrent in the loop, which screens the magnetic flux. Therefore, the phase difference between the superconducting reservoirs is not directly given by the applied magnetic flux. This effect depends on the self-inductance of loop. We will show below, that accounting of this leads to a fully inverted phase dependence and a very good agreement of experimental results and theoretical calculations.

To address the screening effect we consider a superconducting loop interrupted by a weak link. For the

system depicted in Fig. 1 the weak link is the normal metal structure. We therefore have to assume that the entire phase-drop occurs over the normal metal, which is equivalent to say that the critical current in the normal metal (induced by proximity) is smaller than the critical current in the superconducting ring connecting the two reservoirs S1 and S2. The energy of a superconducting loop, containing a weak link reads,

$$E(\varphi) = \frac{1}{2}LI(\varphi)^2 + E_J(\varphi). \quad (4)$$

Here, L is the selfinductance of the loop, which depends on the geometry, and $E_J(\varphi)$ is the Josephson energy of the weak link. It has to be determined from the integration of the current-phase relation $I(\varphi)$. Fluxoid quantization requires that $\varphi = 2\pi\Phi_{\text{tot}}/\Phi_0$ (we restrict ourselves here to $\varphi \in [0, \pi]$, for simplicity). The total flux Φ_{tot} is the sum of the externally applied flux Φ_x and the flux created by the supercurrent $\Phi_{\text{ind}} = LI(\varphi)$. Introducing $\varphi_x = 2\pi\Phi_x/\Phi_0$ and minimizing (4) with respect to φ we obtain an equation, which determines the phase difference as function of the external flux

$$\varphi_x - \varphi = \frac{2e}{\hbar}LI(\varphi) \equiv \gamma I(\varphi). \quad (5)$$

In the limit of vanishing selfinductance ($L \rightarrow 0$) the phase difference across the junction is equal to the externally applied flux. This is usually the desired result. On the other hand, if the left hand side of Eq. (5) is not negligible, the phase at the junction differs from the applied flux. If e.g. the current is $I(\varphi) = I_c \sin \varphi$ and $(2e/\hbar)LI_c \gg 1$, we find $\varphi \approx \varphi_x/(2eLI_c/\hbar) \ll \varphi_x$. The phase is always much smaller than the applied flux. This holds as long as the applied flux is less than π . If the external flux exceeds this value, other solutions become important and the phase jumps. The main consequence of these jumps is, that certain intervals of phases around odd multiples of π can not be reached by modulation of the external flux. Below, we will fully account for the screening, by calculating the full current phase-relation for each temperature. Then the solution of Eq. (5) determines the actual phase difference.

As discussed previously accounting for the screening effect renders a certain interval of phase differences unobservable. Thus, we expect that screening suppresses the resistance at half integer external flux, since the actual phase difference differs from an odd multiple of π . The screening effect is directly seen in the temperature dependence of the resistance for half-integer flux. This is depicted in the right panel Fig. 3 together with the zero-flux resistance. The value of the selfinductance parameter γ is chosen to match the experimentally achieved minimal resistance around 100mK. Note, that without screening the resistance at half-integer flux would be always equal to the normal state resistance. Taking screening into account strongly suppresses the resistance below

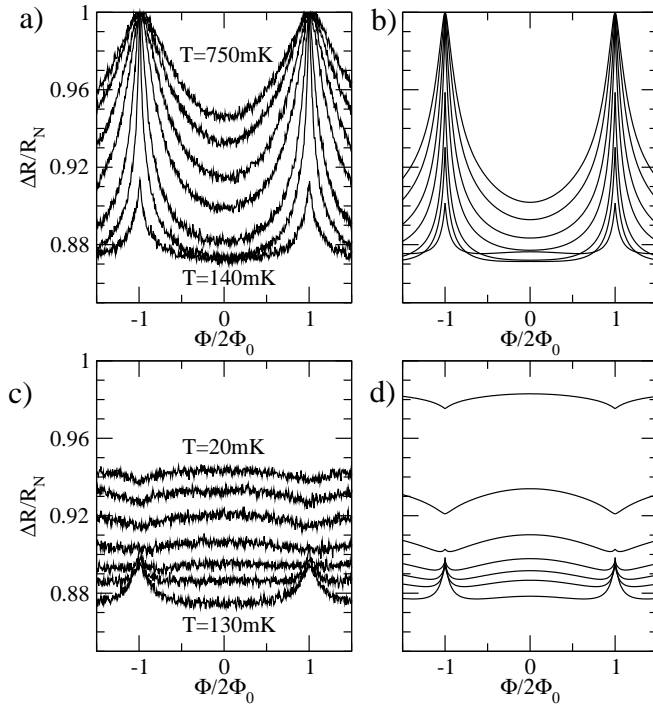


FIG. 4: Resistance oscillations including screening. We compare the theoretical predictions (right column) with the experimental results (left column) using the screening parameter, determined from the fit in Fig. 3. In the upper row the resistance oscillations are compared for temperatures of 750, 600, 450, 350, 250, 200, 140 mK; in the lower row for 130, 105, 95, 85, 70, 50, 20 mK. The agreement is very satisfactory, although not all details coincide.

400mK with a maximal suppression of $\sim 7\%$. At lower temperatures, the resistance reenters, similar as the zero-flux resistance, back to the normal states resistance at zero temperature. As can be seen the resistance for half-integer flux is also slightly below the zero-flux resistance, indicating a reversal of the resistance vs. flux oscillations. This is in agreement with the experimental data. The deviations at high temperatures can be attributed to the neglect of the temperature dependence of the superconducting gap.

To confirm, that the theoretical results are fully consistent with the experimental data, we compare the resistance oscillations for various temperatures in Fig. 4 using the screening parameter, determined from the fit in Fig. 3. The similarity to the experimental curves is quite striking, although not all details coincide. However, it is clearly seen, that the screening effect can lead to the inverted resistance oscillations ("π-shift") at low temperatures, i. e. the system has a negative magnetoresistance.

Let us finally comment on the numerical value of the screening parameter, $\gamma = 0.005e/G_N E_N$. Using the ex-

perimental values $R_N \approx 3\Omega$ and $E_N = 57\text{mK}k_B$, we calculate for the selfinductance of the loop $L \approx 2\text{pH}$. On the other hand, we find for a circular loop of radius $R = 2\mu\text{m}$ and cross section $W^2 = 20 \times 100\text{nm}^2$ a self-inductance $L_{\text{loop}} = \mu_0 R (\ln(8R/W) - 7/4) = 9\text{pH}$. Although the self-inductance of a loop with the experimental geometry is not easy to determine, this rough estimate agrees very well with the selfinductance determined from our fit.

In conclusion we have shown, that a diffusive Andreev interferometer can show a negative magnetoresistance and a non-sinusoidal supercurrent-phase relation. This effect has been calculated theoretically and found experimentally. We obtained excellent agreement with experimental data, if the diamagnetic screening in the superconducting loop imposing the phase difference is taken into account. This eventually leads to a fully inverted ('π-shifted') resistance oscillations.

W. B. was supported by the Swiss NSF and the NCCR Nanoscience.

-
- [1] V. T. Petrashov, V. N. Antonov, P. Delsing, and T. Claesson, JETP Lett. **60**, 606 (1994).
 - [2] H. Pothier, S. Gueron, D. Esteve, and M. H. Devoret, Phys. Rev. Lett. **73**, 2488 (1994).
 - [3] V. T. Petrashov, V. N. Antonov, P. Delsing, and T. Claesson, Phys. Rev. Lett. **74**, 5268 (1995).
 - [4] A. Dimoulas, J. P. Heida, B. J. v. Wees, T. M. Klapwijk, W. v. d. Graaf, and G. Borghs, Phys. Rev. Lett. **74**, 602 (1995).
 - [5] P. Charlat, H. Courtois, , Ph. Gandit, D. Mailly, A. F. Volkov, and B. Pannetier, Phys. Rev. Lett. **77**, 4950 (1996).
 - [6] A. Volkov, N. Allsopp, C. J. Lambert, J. Phys.: Condens. Matter **8**, L45 (1996).
 - [7] Yu. V. Nazarov and T. H. Stoof, Phys. Rev. Lett. **76**, 823 (1996); T. H. Stoof and Yu. V. Nazarov, Phys. Rev. B **54**, R772 (1996).
 - [8] A. A. Golubov, F. K. Wilhelm, and A. D. Zaikin, Phys. Rev. B **55**, 1123 (1997).
 - [9] A. F. Volkov, A. V. Zaitsev, and T. M. Klapwijk, Physica C **59**, 21 (1993).
 - [10] C. J. Lambert and R. Raimondi, J. Phys. Cond. Mat. **10**, 901 (1998).
 - [11] W. Belzig, F. K. Wilhelm, C. Bruder, G. Schön, and A. D. Zaikin, Superlattices Microst. **25**, 1251 (1999).
 - [12] B. Pannetier and H. Courtois, J. of Low Temp. Phys. **118**, 599 (2000).
 - [13] V. N. Antonov, H. Takayanagi, F. K. Wilhelm, and A. D. Zaikin Europhys. Lett. **50**, 250 (2000).
 - [14] A. Kadigrobov, L. Y. Gorelik, R. I. Shekhter, M. Jonson, R. Sh. Shaikhaidarov, V. T. Petrashov, P. Delsing and T. Claesson, Phys. Rev. B **60**, 14589 (1999).
 - [15] Yu. V. Nazarov, Superlattices Microst. **25**, 1221 (1999).
 - [16] G. Eilenberger, Z. Phys. **214**, 195 (1968); A. I. Larkin and Yu. N. Ovchinnikov, Sov. Phys. JETP **26**, 1200 (1968); K. D. Usadel, Phys. Rev. Lett. **25**, 507 (1970).